Published in final edited form as:
Environ Microbiol. 2009 August ; 11(8): 2015–2029. doi:10.1111/j.1462-2920.2009.01923.x.

Identification of a calcium-controlled negative regulatory system affecting *Vibrio cholerae* biofilm formation

Kivanc Bilecen and **Fitnat H. Yildiz***
Department of Microbiology and Environmental Toxicology, University of California, Santa Cruz, Santa Cruz, CA 95064, USA

Summary

Vibrio cholerae 's capacity to cause outbreaks of cholera is linked to its survival and adaptability to changes in aquatic environments. One of the environmental conditions that can vary in *V. cholerae*'s natural aquatic habitats is calcium (Ca^{+2}). In this study, we investigated the response of *V. cholerae* to changes in extracellular Ca^{2+} levels. Whole-genome expression profiling revealed that Ca^{2+} decreased the expression of genes required for biofilm matrix production. Luria–Bertani (LB) medium supplemented with Ca^{2+} ($LBCa^{2+}$) caused *V. cholerae* to form biofilms with decreased thickness and increased roughness, as compared with biofilms formed in LB. Furthermore, addition of Ca^{2+} led to dissolution in biofilms. Transcription of two genes encoding a two-component regulatory system pair, now termed calcium-regulated sensor (*carS*) and regulator (*carR*), was decreased in cells grown in $LBCa^{2+}$. Analysis of null and overexpression alleles of *carS* and *carR* revealed that expression of *vps* (*Vibrio* polysaccharide) genes and biofilm formation are negatively regulated by the CarRS two-component regulatory system. Through epistasis analysis we determined that CarR acts in parallel with HapR, the negative regulator of *vps* gene expression.

Introduction

Vibrio cholerae is a facultative human pathogen and the causative agent of the diarrhoeal disease cholera. The life cycle of this bacterium involves rapid growth within the human intestine and prolonged survival in aquatic habitats (Kaper *et al*., 1995; Faruque *et al*., 1998). *Vibrio cholerae* is a natural inhabitant of coastal and estuarine environments where it is found either as individual cells in the water column or as biofilm-associated cells attached to surfaces (Huq *et al*., 1983; Huq *et al*., 1986; Colwell and Huq, 1994; Huq *et al*., 1995; Islam *et al*., 2007). Indeed, *V. cholerae*'s ability to form biofilms is a key factor for its survival in its natural habitats and transmission to human host.

Production of mature biofilms in *V. cholerae* requires extracellular matrix components. The major component of the *V. cholerae* biofilm matrix is VPS (*Vibrio* polysaccharide) exopolysaccharide, and VPS production is essential for development of 3D biofilm structures (Watnick and Kolter, 1999; Yildiz and Schoolnik, 1999). The extracellular matrix of *V. cholerae* biofilms also contains proteins (RbmA, RbmC and Bap1) that stabilize the biofilm matrix, based on mutant phenotypes (Fong *et al*., 2006; Fong and Yildiz, 2007). Under certain growth conditions, however, *V. cholerae* can also form VPS-independent biofilms (Kierek and Watnick, 2003a,b). This VPS-independent pathway is thought to be preferred in seawater

*For correspondence. yildiz@metx.ucsc.edu; Tel. (+1) 831 459 1588; Fax (+1) 831 459 3524.

Supporting information
Additional Supporting Information may be found in the online version of this article:

environments, and involves intercellular interactions that occur between Ca^{+2} and the O-chain of the outer membrane lipopolysaccharide (LPS) (Kierek and Watnick, 2003a).

The regulatory network that controls biofilm formation by regulating expression of *vps* biosynthesis and matrix protein genes is complex and involves several transcriptional regulators. The core components of this network consist of two positive transcriptional regulators, VpsT and VpsR, and a negative transcriptional regulator HapR (Yildiz and Kolter, 2008). Distruption of *vpsT* reduces *vps* gene expression and impedes biofilm formation (Casper-Lindley and Yildiz, 2004). Disruption of *vpsR*, however, prevents expression of the *vps* genes and production of VPS, and abolishes formation of typical 3D biofilm structure (Yildiz *et al*., 2001; Beyhan *et al*., 2007). Subsequent studies revealed that while VpsR is essential for VPS production and biofilm formation, VpsT plays an accessory role, possibly by increasing the level or activity of VpsR (Beyhan *et al*., 2007). Finally, HapR, the master quorum sensing regulator, negatively regulates biofilm formation in *V. cholerae* (Hammer and Bassler, 2003; Zhu and Mekalanos, 2003; Yildiz *et al*., 2004).

Biofilm formation and dissolution must be tightly controlled to confer a selective advantage to *V. cholerae*. Some environmental signals should therefore trigger biofilm formation, whereas others should inhibit this process and initiate biofilm dissolution. Natural aquatic ecosystems inhabited by *V. cholerae* undergo changes in many physicochemical parameters such as nutrient availability, salinity and temperature (Faruque *et al*., 1998). One of the major environmental fluctuations experienced by *V. cholerae* is altered Ca^{2+} levels. The Ca^{2+} concentration ($[Ca^{2+}]$) in aquatic environments varies from micromolar levels in freshwater to millimolar (~10 mM) levels in marine environments (Riley and Tongudai, 1967).

The known fluctuations in $[Ca^{2+}]$ in *V. cholerae*'s aquatic habitats, and the effect of calcium on VPS-independent biofilm formation (Kierek and Watnick, 2003a) led us to investigate effects of Ca^{2+} on *V. cholerae* and its VPS-dependent biofilms. In this study, we analysed the response and adaptation of *V. cholerae* to an external $[Ca^{2+}]$ increase. We determined that Ca^{2+} negatively regulates transcription of genes that are involved in VPS-dependent biofilm formation. We also identified a two-component regulatory system (now termed calcium-regulated sensor (CarS) and regulator (CarR)), whose transcription decreases in response to an external $[Ca^{2+}]$ increase. Mutational and phenotypic analysis of these regulatory genes revealed that the CarRS two-component regulatory system negatively regulates *vps* gene expression and biofilm formation in *V. cholerae*. Epistasis analysis further showed that CarR and HapR act in parallel pathways to negatively regulate biofilm formation in *V. cholerae*.

Results

Transcriptome response of *V. cholerae* cells to an increase in external $[Ca^{2+}]$

To identify genes that are regulated by Ca^{2+}, we compared whole-genome expression profiles of the wild-type *V. cholerae* cells grown in Luria–Bertani (LB) medium alone and in LB medium supplemented with 10 mM $CaCl_2$ ($LBCa^{2+}$) to mimic high Ca^{2+} levels of marine environments. Gene expression data were analysed using the Significance Analysis of Microarrays (SAM) program. We applied the following criteria to define significantly regulated genes: ≤ 3% false discovery rate and ≥ 1.5-fold transcript abundance differences between the samples. Using the selection criteria given above, a total of 76 genes were found to be differentially regulated in cells grown in $LBCa^{2+}$ compared with the cells grown in LB. Seventeen of these genes were induced and 59 were repressed in Ca^{2+}-adapted cells, as compared with those grown in LB (Table S1). Genes required for different cellular processes including virulence, iron acquisition, biofilm formation and transcriptional regulation were regulated by Ca^{2+} (Table 1 and Table S1). In this study, however, we focused on two sets of

genes: the ones involved in biofilm formation and the ones predicted to be transcriptional regulators.

Ca^{2+} decreased the message abundance of many of the genes encoding proteins required for VPS biosynthesis (Table 1). VPS biosynthesis genes (*vps*) are clustered in two regions on the large chromosome of *V. cholerae* O1 El Tor [*vps*U (VC0916), *vpsA-K*, VC0917-27 (*vps*-I cluster); *vpsL-Q*, VC0934-9 (*vps*-II cluster)]. This result was confirmed by determining β-galactosidase activity in *V. cholerae* carrying *lacZ* transcriptional fusions to the promoter of the first genes in the predicted *vps*-I (*vpsA–lacZ*) and *vps*-II operons (*vpsL–lacZ*). Cells grown in $LBCa^{2+}$ exhibited a threefold decrease in *vpsA–lacZ* and fourfold decrease in *vpsL–lacZ* β-galactosidase activities, relative to cells grown in LB (Fig. 1A). Transcription of the *vps* genes is positively regulated by the transcriptional regulators VpsT and VpsR (Yildiz *et al*., 2001;Casper-Lindley and Yildiz, 2004). Analysis of the expression profiling results revealed that the expression of *vpsR* is decreased in cells grown in $LBCa^{2+}$ compared with those grown in LB. This result was confirmed by determining β-galactosidase activity in wild-type cells carrying *lacZ* transcriptional fusions to the promoter of the *vpsR*; transcription of *vpsR* decreased by 2.8-fold (Fig. 1A). We determined that transcription of *vpsT* is also decreased by 2.3-fold in cells grown in $LBCa^{2+}$ (Fig. 1A). Taken together, these results indicate that decreased *vps* gene expression in cells grown in $LBCa^{2+}$ could be due to decreased transcription of the *vpsR* and *vpsT* genes.

Ca^{2+} and biofilm development

A major component of *V. cholerae* biofilm matrix is VPS, which is essential for the development of mature biofilm structures (Watnick and Kolter, 1999; Yildiz and Schoolnik, 1999). Because Ca^{2+} affected the message abundance of the *vps* genes, we analysed the effect of Ca^{2+} on biofilm formation. We compared structure of biofilms, formed by wild-type cells grown in LB to those grown in $LBCa^{2+}$ using a flow-cell system (Fig. 1B).

Quantitative analysis of these biofilm images revealed that Ca^{2+} significantly altered biofilm structure (Fig. 1C). While biofilms grown in LB had increased average biofilm thickness, their maximum thickness values were similar (Fig. 1C). Biofilm roughness, a measure of biofilm thickness heterogeneity, was greater for biofilms grown in $LBCa^{2+}$ compared with biofilms grown in LB, indicating that the surface architecture of the LB biofilms is more regular (Fig. 1C).

We reasoned that the stability of biofilms grown in LB and $LBCa^{2+}$ could also be different. To test this possibility, we treated 48-hour-old biofilms grown in $LBCa^{2+}$ and in LB with 0.5% SDS for 15 min, and determined biofilm structures. SDS addition led to higher dissolution in biofilms grown in $LBCa^{2+}$, indicating that biofilms grown in $LBCa^{2+}$ were less stable compared with biofilms grown in LB (Fig. 1B). Lower *vps* gene expression at high $[Ca^{2+}]$ – resulting in a decrease in VPS production – is the likely cause of this instability. An alternative explanation is that interactions between Ca^{+2} and the O-chain of the outer membrane LPS or biofilm matrix proteins lead to changes in biofilm stability.

To evaluate the importance of VPS to Ca^{2+}-mediated changes to biofilm structure and stability, we tested the effect of an increased $[Ca^{2+}]$ on biofilms of a mutant that is unable to produce VPS, due to deletion of *vps*-I and *vps*-II clusters (Δ*vps*-IΔ*vps*-II, called Δ*vps*). Biofilms of the Δ*vps* mutant consisted of flat monolayers of cells; thus, the effect of Ca^{2+} on biofilm thickness and roughness due to VPS production cannot be evaluated. Hence, we looked at SDS mediated detachment of biofilms. Biofilms of Δ*vps* mutants detached readily from the substratum upon treatment with 0.5% SDS (Fig. 1D). These results indicate that VPS is necessary for biofilm stability. Interestingly, however, Ca^{2+} addition to Δ*vps* biofilms led to detachment, decrease in substratum coverage and formation of clusters of microcolonies (Fig. 1D and E). Such

aggregates were also present in wild-type biofilms grown in LBCa^{2+} (Fig. 1B). Together, these observations suggest that Ca^{2+} addition alters either cell-cell or cell–surface interactions to create more clustered but less well attached biofilms. This finding also suggests that there are other factors besides VPS that are involved in calcium-mediated changes in biofilm structure. This observation is consistent with the report that *V. cholerae* can form VPS-independent biofilms that require interactions between Ca^{+2} and the O-chain of the outer membrane LPS (Kierek and Watnick, 2003a).

We also analysed the effect of [Ca^{2+}] on preformed biofilms in two different ways. In the first set of flow-cell experiments, biofilms were grown in LB for 24 h then the media was supplemented with 10 mM Ca^{2+}, and biofilms were analysed after 24 h of incubation (Fig. S1A). Quantitative analysis of these biofilm images revealed that Ca^{2+} significantly altered the architecture of biofilms (Fig. S2A). Ca^{2+} addition to preformed biofilms decreased the average biofilm thickness and increased biofilm roughness. It is noteworthy that the analysis of the effect of Ca^{2+} addition on biofilms grown in defined artificial sea water-based medium also revealed similar results (Fig. S1C). In the second set of experiments, we analysed the effect of Ca^{2+} removal on biofilms grown in LBCa^{2+} for 24 h (Fig. S1B). In this case, while the mean thicknesses decreased, surface coverage dramatically increased in the biofilms 24 h after the removal of Ca^{2+} from the biofilm medium (Fig. S2B). This decrease in biofilm thickness is most likely due to the increased compactness of biofilms with an increase in VPS and biofilm matrix protein productions. Collectively, these studies clearly showed that the structural properties of biofilms formed in LBCa^{2+} are different than those formed in LB.

Regulators of biofilm formation and Ca^{2+} response

Transcriptional regulators, VpsR and VpsT positively regulate VPS production and biofilm formation. Because our microarray data above suggested that [Ca^{2+}] affects *vps* gene expression, we wanted to further analyse how VpsR and VpsT are involved in Ca^{2+}-mediated repression of *vps* gene expression. To this end, we introduced a plasmid harbouring a *vpsL–lacZ* transcriptional fusion into Δ*vpsR* and Δ*vpsT* mutants, and measured *vpsL* transcription in cells grown in LB and LBCa^{2+}. No *vpsL* transcription was detected in *vpsR* mutant cells grown in either LB or LBCa^{2+}, as expected (Fig. 2). The *vpsT* mutant exhibited a 3.7-fold decrease in *vpsL* expression, compared with that of the wild-type cells grown in LB (Fig. 2). Wild-type cells showed an approximately fivefold difference of *vpsL* expression between cells grown in LB or LBCa^{2+}, the *vpsT* mutant showed a threefold difference, and the *vpsR* mutant showed essentially no *vpsL* expression. This finding suggests that the Δ*vpsT* strain is still able to respond to an increase in external Ca^{2+} levels.

The quorum sensing regulator, HapR, was previously shown to negatively regulate transcription of *vps* genes (Hammer and Bassler, 2003; Zhu and Mekalanos, 2003; Yildiz *et al*., 2004). To determine whether this regulator was important for Ca^{2+}-mediated repression of *vps* gene expression, we also analysed *vpsL* expression in a Δ*hapR* mutant grown in LB and LBCa^{2+}. Similar to the wild-type, *vpsL* expression decreased in cells grown in LBCa^{2+} (Fig. 2), indicating that HapR does not regulate *vps* expression in a Ca^{2+}-dependent manner.

Ca^{2+} regulates transcription of genes encoding a two-component regulatory pair

Comparison of whole-genome expression profiles of the cells grown in LBCa^{2+} to cells grown in LB medium revealed that Ca^{2+} leads to a decrease in transcription of genes predicted to encode proteins with regulatory functions (i.e. VC1319, encoding a sensor histidine kinase, and VC1320, encoding a response regulator). Message abundance of VC1319 and VC1320 were decreased by 1.6-fold and 2.3-fold respectively (Table 1 and Table S1). We also made the same observation when we analysed the initial response of *V. cholerae* to an increase in external [Ca^{2+}] by monitoring changes in the gene expression profile in exponentially grown

cells that were subjected to 'Ca^{2+} addition' for 15 and 30 min (Table S1). We named VC1319 '*carS*' for calcium regulated sensor histidine kinase and VC1320 '*carR*' for calcium regulated response regulator.

The *carS* gene is predicted to encode a 440-aminoacid, 50.2 kDa protein that exhibits 27.1% identity/46.0% similarity to *Escherichia coli* RstB. The *carR* gene is predicted to encode a 234-amino-acid, 26.4 kDa protein that exhibits 44.6% identity/63.6% similarity to *E. coli* RstA. The RstAB two-component regulatory pair is part of the divalent cation-sensing PhoPQ regulon (Minagawa *et al*., 2003; Ogasawara *et al*., 2007); however, the environmental stimuli required for the activation of RstAB are unknown (Eguchi *et al*., 2004).

To confirm the expression profile data, we constructed *carR–lacZ* transcriptional fusion (*carS* and *carR* are separated by 25 bp and predicted to be organized in an operon where *carR* is the first gene) by amplifying the upstream regulatory sequence of *carR*, and inserting it into the upstream of a promoterless *lacZ* gene in vector pRS415. Transcription was measured by determining β-galactosidase activity in wild-type cells grown in LB and LBCa^{2+}. Cells grown in LBCa^{2+} exhibited a decrease in β-galactosidase activity relative to cells grown in LB (Fig. 3A), confirming the trend of the microarray experiment.

CarS and CarR negatively regulate vps gene expression

As we determined that expression of both *vps* and *carRS* genes are negatively regulated in cells treated with Ca^{+2}, we wanted to determine whether CarRS is involved in Ca^{2+}-mediated repression of *vps* genes. To this end, we generated in-frame deletion mutants of *carS* and *carR*. To identify genes regulated by CarS and CarR, we first compared whole-genome expression profiles of the Δ*carS* and Δ*carR* mutants to the wild-type using total RNA isolated from cells grown in LB. Gene expression data were analysed using the SAM program with the criteria discussed above. We found a total of 19 differentially regulated genes in Δ*carS* compared with the wild-type during exponential phase. Of these genes, 9 were induced and 10 were repressed in Δ*carS* compared with the wild-type (Table S1 and Fig. S3). In the Δ*carR* mutant, 67 genes were differentially expressed; of which 27 were induced and 40 were repressed compared with the wild-type (Table S1 and Fig. S3).

Interestingly, expression profiling showed that mRNA abundance of many of the *vps* and *vps* intergenic region genes were increased in the Δ*carR* mutant by 1.5- to 2.7-fold relative to the wild-type. Similarly, mRNA levels from some of the *vps* genes (VC0918, VC0933 and VC0935) were also increased in the Δ*carS* mutant relative to the wild-type. This result was confirmed by determining β-galactosidase activity in strains harbouring plasmids with *vpsA–lacZ* and *vpsL–lacZ* transcriptional fusions. Transcription of both *vpsA* and *vpsL* was increased in the Δ*carS* and Δ*carR* mutants relative to the wild-type (Fig. 3B). Taken together, these results suggest that CarR and CarS negatively regulate *vps* gene expression.

To better evaluate the mechanism by which CarR negatively regulates *vps* expression, we analysed *vpsT* and *vpsR* transcription in the wild-type and Δ*carR* strains harbouring *vpsT–lacZ* and *vpsR–lacZ* fusion plasmids (Fig. 3C). A 2- and 1.4-fold increase in β-galactosidase activities was observed in Δ*carR* harbouring *vpsT–lacZ* and *vpsR–lacZ* fusion plasmids, respectively, when compared with the wild-type. These results suggest that CarR negatively regulates the expression of both *vpsT* and *vpsR*, and that increased *vps* expression in Δ*carR* could be due to increased transcription of the *vpsR* and *vpsT* genes.

To further evaluate contributions of CarS and CarR to Ca^{2+} adaptation response, we also determined the whole-genome transcriptional profile of Δ*carS* and Δ*carR* mutants upon an increase in [Ca^{2+}]. In large part, Ca^{2+} adaptation responses of these mutants were similar to

those of the wild-type (Fig. S3). This observation indicates that the CarRS regulatory system regulates expression of only a small set of genes that is regulated by external [Ca^{2+}] increase.

To confirm that the CarRS system is not involved in the Ca^{2+} regulation of the *vps* genes, we compared *vpsA* and *vpsL* expressions in the wild-type, Δ*carS* and Δ*carR* strains grown in LB and LBCa^{2+}. Expression of *vpsA* and *vpsL* genes was higher in Δ*carS* and Δ*carR* mutants relative to wild-type when grown in LB or LBCa^{2+}. However, we found decreased β-galactosidase activities in the wild-type, Δ*carS* and Δ*carR* strains grown in LBCa^{2+}, relative to cells grown in LB (Fig. 3D). These results are consistent with microarray results, showing that the CarRS two-component regulatory system is not involved in Ca^{2+}-mediated repression of *vps* gene expression.

Taken together, our results suggest that in Ca^{2+}-treated cells there appears to be two parallel signalling pathways controlling *vps* gene expression. In the first pathway transcription of *vpsR* and *vpsT*, and in turn *vps* structural genes, is decreased by a yet to be determined mechanism. The second pathway is controlled by CarR, where a decrease in the transcription of *carR* would lead to an increase in the transcription of *vpsR*, *vpsT* and *vps* genes (Fig. 3). Because Ca^{2+}-treated wild-type cells have decreased *vps* expression, the first pathway appears to be dominant over CarRS-dependent pathway.

CarS and CarR affect biofilm formation

CarS and CarR negatively regulate transcription of *vps* genes; therefore, Δ*carS* and Δ*carR* mutants are expected to have altered biofilm structures. To test this idea, we compared the biofilms of the Δ*carS* and Δ*carR* mutants to the wild-type biofilms. We first analysed biofilms formed on chambered coverglasses after 8 h of incubation under static conditions at 30°C, with biofilm structures analysed by confocal scanning laser microscopy (CSLM). The results, shown in Fig. 4A, revealed that both Δ*carS* and Δ*carR* mutants have an enhanced capacity to form biofilms. To gain further insight into the structure of biofilms formed by the Δ*carS* and Δ*carR* mutants, biofilms were grown at room temperature in flow cells for 48 h (Fig. 4B). Biofilms formed by the Δ*carS* and Δ*carR* mutants had higher average thickness and had more pillar-like structures relative to the wild-type biofilms (Fig. 4B and Table 2).

To further evaluate the effect of CarS and CarR on biofilm formation, we overexpressed *carS* and *carR* from an arabinose-inducible vector in wild-type cells (Fig. 4C). Biofilms of cells harbouring *carR* and *carS* overexpression plasmids were grown in a flow-cell system, using LB medium supplemented with 0.2% arabinose, with images acquired by CSLM over the course of the biofilm development (Fig. 4C). There was a significant difference in biofilm formation dynamics in cells overexpressing CarR, relative to the control strain. In cells overexpressing CarR, surface attachment and surface coverage were decreased dramatically 8 and 24 h after the inoculation (Fig. 4C and Table 2). Although strains overexpressing CarS exhibited a decrease in surface coverage, the defect was less profound than that seen with CarR overexpression. After 48 h of biofilm development, strains overexpressing CarS and CarR were able to form biofilms. However, final biofilm architecture and surface colonization were different than in the biofilms of the control strain. Taken together, our studies indicate that the CarRS regulatory system negatively regulates biofilm formation in *V. cholerae*.

Epistasis analysis of carR, vpsR, vpsT and hapR

VpsR is the most downstream regulator of *vps* gene transcription in the VpsT, VpsR and HapR regulatory circuitry (Beyhan *et al*., 2007). To determine how CarR contributes to this regulatory circuitry, we generated Δ*carR*Δ*vpsR*, Δ*carR*Δ*vpsT* and Δ*carR*Δ*hapR* double mutants. We then monitored transcription of the *vpsL–lacZ* fusion in wild-type, Δ*carR*, Δ*vpsT*, Δ*vpsR*, Δ*carR*Δ*vpsT* and Δ*carR*-Δ*vpsR* mutants (Fig. 5A). As discussed above, in Δ*carR* mutant the

transcription of *vpsL* is markedly increased compared with the wild-type. Transcription of *vpsL–lacZ* is decreased in Δ*vpsT* and Δ*vpsR* by 2.5-fold and 57.5-fold, respectively, compared with the wild-type (Fig. 5A). While v*psL* expression was similar in the Δ*vpsR* and Δ*carR*-Δ*vpsR* strains, indicating that VpsR acts downstream of CarR. v*psL* expression was 2.6-fold higher in the Δ*carR*-Δ*vpsT* mutant relative to that of the Δ*vpsT* mutant, indicating that VpsT and CarR act on parallel pathways. We reported previously that VpsT positively regulates transcription of *vpsR* (Casper-Lindley and Yildiz, 2004). Hence, the decrease in *vpsL* transcription in the Δ*carR*-Δ*vpsT* strain is likely due to decreased expression of *vpsR*.

Biofilm formation in *V. cholerae* is negatively regulated by HapR. To determine a possible connection between CarR and HapR, we monitored transcription of *vpsL*, using *lacZ* transcriptional fusion constructs in wild-type, Δ*carR,* Δ*hapR* and Δ*carR*Δ*hapR* mutants (Fig. 5A). Transcription of *vpsL–lacZ* was increased in Δ*carR* and Δ*hapR* by 3- and 10-fold, respectively, compared with the wild-type (Fig. 5A). Transcription of *vpsL–lacZ* was higher in the Δ*carR*Δ*hapR* strain than in the Δ*hapR* strain, indicating that CarR and HapR act in parallel pathways to negatively regulate *vps* gene expression (Fig. 5A).

Discussion

In bacteria, relatively little is known about Ca^{2+} signalling and the processes that are regulated by Ca^{2+} (reviewed in Norris *et al*., 1991; Norris *et al*., 1996; Dominguez, 2004). Intracellular [Ca^{2+}] in bacterial cells is dynamic, and changes in intracellular [Ca^{2+}] could regulate diverse cellular processes (reviewed in Norris *et al*., 1991; Norris *et al*., 1996; Dominguez, 2004). Intracellular [Ca^{2+}] measurements in *E. coli* revealed that [Ca^{2+}] ranges from 170 to 300 nM (Jones *et al*., 1999). Furthermore, intracellular Ca^{2+} levels were found to vary as a function of external Ca^{2+} levels, reaching approximately 2 μM upon exposure to 1 mM external [Ca^{2+}] (Holland *et al*., 1999). Intracellular Ca^{2+} levels in bacteria are controlled by influx mechanisms through the actions of ion channels, primary and secondary transporters, Ca^{2+} export systems and Ca^{2+}-binding proteins (CaBP) (Norris *et al*., 1996; Jones *et al*., 1999). Because *V. cholerae* is predicted to experience [Ca^{2+}] fluxes in its environment, we reasoned that it might respond to changes in external [Ca^{2+}]. In this study, we determined that an increase in [Ca^{2+}] leads to a decrease in *vps* gene expression and VPS-dependent biofilm formation in *V. cholerae*.

Ca^{2+} has been shown to influence surface attachment and biofilm formation in other bacteria. The role of Ca^{2+} can be due to its bridging role in the extracellular polymeric matrix (Rose and Turner, 1998; Rose, 2000), its interactions with extracellular or cell surface-associated Ca^{2+}-binding proteins (Arrizubieta *et al*., 2004), or its regulatory effects on the expression of genes known to play roles in biofilm formation and surface attachment. A proteomic analysis, designed to elucidate cellular response to an increase in external [Ca^{2+}] in the marine bacterium *Pseudoalteromonas* sp. 1398, revealed that an increase in [Ca^{2+}] caused a global change in the protein expression profile during both planktonic and biofilm-mode of growth (Patrauchan *et al*., 2005). Furthermore, an increase in [Ca^{2+}] was found to enhance extracellular matrix production. In *Pseudomonas aeruginosa*, an increase in [Ca^{2+}] induces transcription of alginate biosynthesis genes and the amount of alginate in biofilm matrix (Sarkisova *et al*., 2005). In contrast, we observed that in *V. cholerae* VPS-dependent extracellular matrix production is decreased in response to an increase in [Ca^{2+}]. In *Staphylococcus aureus* strains, harbouring the biofilm-associated protein Bap, elevated extracellular calcium levels inhibited intercellular adhesion and biofilm formation (Arrizubieta *et al*., 2004). Bap is a staphylococcal surface protein that is involved in biofilm formation and binds Ca^{2+} via an EF-hand motif (Gotz, 2002). It was shown that Bap binds Ca^{2+} with low affinity and, upon Ca^{2+} binding, Bap loses its ability to promote biofilm formation (Arrizubieta *et al*., 2004). Our lab has recently identified a set of biofilm matrix proteins, and two of these proteins, RbmC and Bap1, also

harbour a Ca^{2+}-binding domain (Fong and Yildiz, 2007). We are currently testing whether these proteins bind Ca^{2+} and how these interactions affect *V. cholerae* biofilm formation.

The mechanism by which *V. cholerae* senses external [Ca^{2+}] is not known. In *Salmonella*, a two-component regulatory system, PhoPQ, is required for sensing divalent cations (Ca^{2+}, Mg^{2+}, Mn^{2}), antimicrobial peptides and acidity. The PhoPQ system is active at low divalent cation concentrations, and under such conditions the membrane-localized sensor histidine kinase, PhoQ, auto-phosphorylates and then phosphorylates its cognate response regulator, PhoP (reviewed in Groisman, 2001; Prost and Miller, 2008). The phosphorylated PhoP activates transcription of several genes required for virulence. *Vibrio cholerae* genome analysis revealed that there are putative PhoPQ homologues (VCA1104-05 and VC1638-39) in the genome, which may be involved in sensing divalent cations, and we are currently analysing their roles in Ca^{2+} sensing.

In this study, we also identified a set of transcriptional regulators, CarS and CarR, whose expression is down-regulated under increased [Ca^{2+}] conditions. We determined that CarR and CarS negatively regulates *vps* gene expression and biofilm formation in *V. cholerae*. These proteins are homologous to RstB and RstA of *E. coli* respectively. In *E. coli*, the *rstAB* operon was originally identified as part of the PhoPQ two-component regulatory system. Because CarRS is homologous to RstAB, our findings together suggest that a PhoPQ-like signal transduction system is also operational in *V. cholerae*. Phenotypic analysis of the *rstAB* mutant, using phenotype microarrays, revealed that RstAB is involved in resistance to antibiotics ketoprofen, pridinol and troleandomycin (Zhou *et al*., 2003). To date, two genes, *asr* and *csgD*, have been shown to be under the control of RstA (Ogasawara *et al*., 2007). *asr* is needed for the survival of *E. coli* in a low-pH environment (Seputiene *et al*., 2003). The second gene that is regulated by RstA is *csgD,* encoding a transcription factor that is required for the production of biofilm matrix components in *E. coli* and *Salmonella* spp. (Romling *et al*., 1998). RstAB negatively regulates CsgD expression and therefore biofilm formation in *E. coli* (Ogasawara *et al*., 2007). Our results showed that in *V. cholerae* the CarRS two-component system negatively regulates the expression of *vpsT*, which exhibits 44% sequence identity to CsgD, the positive regulator of *vps* gene expression and biofilm formation (Casper-Lindley and Yildiz, 2004). Our analysis also revealed that CarRS positively regulates transcription of genes predicted to be involved in lipid A modification (Table S1). It is not known if RstA is involved in such a response, but PhoPQ regulates structural modifications to lipid A in *Salmonella* spp., and such modifications play a role during infection, mediating resistance to host antimicrobial peptides and avoidance of immune system.

In this study, we showed that extracellular [Ca^{2+}] is an environmental signal that negatively affects VPS-dependent biofilm formation and identified a calcium-controlled negative regulatory system affecting *V. cholerae* biofilm formation. Better understanding of responses of *V. cholerae* to the physical and chemical factors that are likely to be encountered by the pathogen in natural aquatic habitats, as well as the environmental signals and regulatory networks that govern transitions between planktonic and biofilm states of *V. cholerae* in aquatic ecosystems, will shed light on the mechanism of survival of the organism in the environment and transmission to human host.

Experimental procedures

Bacterial strains and growth conditions

Bacterial strains and plasmids used in this study are listed in Table 3. Luria–Bertani broth (1% Tryptone, 0.5% Yeast Extract and 1% NaCl) at pH 7.0 or LB supplemented with 10 mM $CaCl_2$ (LBCa^{2+}) at pH 7.0 were used. *Vibrio cholerae* cultures were grown in LB or LBCa^{2+} at 30°C to an OD_{600} of 0.3 (corresponding to ~2×10^8 cells ml^{-1}) in 125 ml flasks containing

25 ml of growth medium and were shaken at 200 r.p.m. *Escherichia coli* cultures were grown at 37°C in LB and were shaken at 200 r.p.m. Under this condition, growth kinetics of *V. cholerae* cells grown in LB or LBCa^{2+} are nearly identical (data not shown). Unless otherwise noted, the antibiotics rifampicin (Rif) and ampicillin (Amp) were added at concentrations of 100 μg ml^{-1}, and gentamicin was added at concentration of 50 μg ml^{-1}. LB broth without NaCl and with 10% sucrose was used for counter selection with *sacB*-containing plasmids. Arabinose, 0.2% (w/v), was used for induction of gene expression and was added to the growth medium when necessary. The salt base of ASW used in biofilm assays contained 9.25 mM $CaCl_2$, 8.32 mM KCl, 23.12 mM $MgCl_2 \cdot 6H_2O$, 52.34 mM $MgSO_4$, 422.66 mM NaCl, 2.14 mM $NaHCO_3$, 0.07 mM NaF, 0.747 mM KBr, 0.388 mM H_3BO_3 and 0.15 mM $SrCl_2$. The (ASW) salt base was supplemented with 0.005% K_2HPO_4, 0.1% NH_4Cl, 10 mM 4-(2-hydroxyethyl)-1-piperazineethanesulfonic acid (Hepes), 1× MEM Vitamin Solution (Gibco-Invitrogen), 0.2% peptone and 0.01% yeast extract.

DNA manipulations, generation of deletion mutants and green fluorescent protein (*gfp*) tagging of *V. cholerae* strains

All oligonucleotides used for PCR analysis and DNA sequencing were obtained from Operon Technologies (Alameda, CA) and are listed in Table S2. All PCRs were performed with the High-Fidelity or Expand High-Fidelity PCR kits (Roche). PCR products and plasmids were cleaned and prepared using QiaQuick PCR purification (QIAGEN), QiaPrep Spin Miniprep (QIAGEN) and GFX PCR DNA Gel Band Purification (GE Healthcare) kits. DNA sequencing was done at the UC Berkeley DNA Sequencing Facility.

Deletions for all genes were carried out using the same general strategy, as described in Lim and colleagues (2006). Briefly, a ~600 bp fragment 5′ of the gene, including several nucleotides of the gene, was amplified by PCR with primers A and B (Table S2). A similar fragment was also amplified from the 3′ end of the gene, using primers C and D (Table S2). Purified PCR fragments from these reactions were allowed to anneal to sequences in primers B and C and amplified in a second PCR reaction. The resulting ~1200 bp fragment was then amplified with primers A and D, creating the deletion construct. The purified PCR fragment was digested with two of the following restriction enzymes: SacI, NcoI or XbaI, and ligated into a pGP704-*sacB*28 suicide plasmid digested with the same enzymes. The deletion constructs are listed in Table 3. The deletion plasmids were maintained in *E. coli* CC118 (λ *pir*). Biparental matings were carried out with the wild-type *V. cholerae* and a conjugative strain *E. coli* S17-1 (λ *pir*) harbouring deletion plasmid. Selection of deletion mutants were done as described by Fong and Yildiz (2007) and were verified by PCR. The *gfp*-tagged *V. cholerae* strains were generated by triparental matings with donor *E. coli* S17-1 (λ *pir*) carrying pMCM11, helper *E. coli* S17-1 (λ *pir*) harbouring pUX-BF13 and *V. cholerae* strains. Transconjugants were selected on thiosulfate-citrate-bile salts-sucrose (Difco) agar medium containing gentamicin at 30°C. The *gfp*-tagged *V. cholerae* strains were verified by PCR.

RNA isolation and whole-genome expression profiling

Total RNA was isolated from *V. cholerae* cells grown in LB medium to an OD_{600} of 0.3–0.4. RNA isolation was done as described by Beyhan and colleagues (2007). To analyse the initial response to an increase in external [Ca^{+2}], a final concentration of 10 mM Ca^{2+} was added to exponentially grown cells and cells were collected 15 and 30 min after Ca^{2+} addition. To analyse adaptation to an increase in external [Ca^{+2}], overnight grown cultures of *V. cholerae* in LB medium at 30°C were diluted 1:200 in LBCa^{2+} and incubated at 30°C with shaking (200 r.p.m), until they reached to an OD_{600} of 0.3–0.4. To ensure homogeneity, these cultures were diluted again 1:200 in LBCa^{2+} medium and grown to an OD_{600} of 0.3–0.4. Aliquots of 1.8 ml were collected by centrifugation for 2 min at room temperature. The cell pellets were immediately resuspended in 1 ml of Trizol reagent (Invitrogen) and stored at −80°C. The total

RNA from the pellets was isolated according to the manufacturer's instructions. To remove contaminating DNA, total RNA was incubated with RNase-free DNase I (Ambion), and the RNeasy Mini kit (QIAGEN) was used to clean up the RNA after DNase digestion.

Microarrays used in this study were composed of 70-mer oligonucleotides, representing the open reading frames present in *V. cholerae* genome. These were designed and synthesized by Illumina, San Diego, and printed at UCSC. Whole-genome expression analysis was performed using a common reference, which was RNA-isolated from wild-type strains grown to an OD_{600} of 0.3–0.4. RNA samples from test and reference samples were used in cDNA synthesis, and microarray hybridization and scanning were performed as described previously (Beyhan *et al*., 2006; 2007). Normalized signal ratios were obtained with LOWESS print-tip normalization, using the Bioconductor packages (http://www.bioconductor.org) in an R environment. Differentially regulated genes were determined (with 3 biological and 2 technical replicates for the analysis of Ca^{2+} adaptation and Δ*carR/S* regulation or, 2 biological and 2 technical replicates for identification of initial Ca^{2+} response and the Δ*carR/S* response to Ca^{2+}) using the SAM software (Tusher *et al*., 2001), with a 1.5-fold difference in gene expression and a 3% false discovery rate as a cutoff value. Identification of genes with similar expression pattern was performed by analysing the data using GENESIS software (Sturn *et al*., 2002).

β-Galactosidase assays

Overnight grown cultures of *V. cholerae* in LB medium at 30°C were diluted 1:200 in either LB or LBCa^{2+} and incubated at 30°C with shaking (200 r.p.m), until they reached to an OD_{600} of 0.3–0.4. To ensure homogeneity, these cultures were diluted again 1:200 in appropriate medium and grown to an OD_{600} of 0.3–0.4. Cell harvesting and β-galactosidase assays were carried out according to a previously published procedure (Fong *et al*., 2006). The assays were repeated with three different biological replicates and at least eight technical replicates.

Biofilm assays

Biofilms were grown either at room temperature in flow cells (individual channel dimensions of 1 × 4 × 40 mm) or at 30°C in chambered cover-slides. Biofilms in flow cells were supplied with 2% LB (0.01% yeast extract, 0.02% tryptone and 1% NaCl) or ASW at a flow rate of 10.2 ml h^{-1}. The flow-cell system was assembled and prepared as described previously (Heydorn *et al*., 2000). Cultures for inoculation of the flow cells were prepared by inoculating a single colony from a plate into flasks containing LB medium and growing them with aeration at 30° C for 16 h. Cultures were diluted to an OD_{600} of 0.1 in 2% LB and used for inoculation. A 300 μl volume of diluted culture was injected into each chamber with a small syringe. After inoculation, flow cells were left at room temperature for 1 h without flow. The flow was then started at a constant rate of 10.2 ml h^{-1} with a Watson Marlow 205S peristaltic pump. Static biofilms were formed in chambered cover-slides at 30°C. Cultures for inoculation of the chambered cover-slides were grown as described above. Cultures were diluted to an OD_{600} of 0.02 in LB and 3 ml of this dilution was used for inoculation. Three millilitres of 0.5% SDS in 0.9% NaCl was administered into flow cells at 48 h time point to test biofilm stability. Biofilms were incubated for 15 min without flow, and then the flow reinstated and biofilms were incubated for another 15 min in the presence of appropriate growth medium. Confocal scanning laser microscopy images of the biofilms were captured with a LSM 5 PASCAL system (Zeiss) at 488 nm excitation and 543 nm emission wavelengths. Three-dimensional images of the biofilms were reconstructed using Imaris software (Bitplane). Images from each experiment were analysed using the computer program COMSTAT (Heydorn *et al*., 2000) in MATLAB environment.

Supplementary Material

Refer to Web version on PubMed Central for supplementary material.

Acknowledgments

This work was supported by grants from NIH (RO1 AI055987) and CEQI0047 provided by the UC Marine Council Coastal Environmental Quality Initiative. We thank Karen Ottemann, Chad Saltikov, Manel Camps and members of the Yildiz laboratory for their suggestions.

References

Arrizubieta MJ, Toledo-Arana A, Amorena B, Penades JR, Lasa I. Calcium inhibits bap-dependent multicellular behavior in *Staphylococcus aureus*. J Bacteriol 2004;186:7490–7498. [PubMed: 15516560]

Bao Y, Lies DP, Fu H, Roberts GP. An improved Tn7-based system for the single-copy insertion of cloned genes into chromosomes of gram-negative bacteria. Gene 1991;109:167–168. [PubMed: 1661697]

Beyhan S, Tischler AD, Camilli A, Yildiz FH. Transcriptome and phenotypic responses of *Vibrio cholerae* to increased cyclic di-GMP level. J Bacteriol 2006;188:3600–3613. [PubMed: 16672614]

Beyhan S, Bilecen K, Salama SR, Casper-Lindley C, Yildiz FH. Regulation of rugosity and biofilm formation in *Vibrio cholerae*: comparison of VpsT and VpsR regulons and epistasis analysis of *vpsT*, *vpsR*, and *hapR*. J Bacteriol 2007;189:388–402. [PubMed: 17071756]

Casper-Lindley C, Yildiz FH. VpsT is a transcriptional regulator required for expression of *vps* biosynthesis genes and the development of rugose colonial morphology in *Vibrio cholerae* O1 El Tor. J Bacteriol 2004;186:1574–1578. [PubMed: 14973043]

Colwell RR, Huq A. Environmental reservoir of *Vibrio cholerae*. The causative agent of cholera. Ann NY Acad Sci 1994;740:44–54. [PubMed: 7840478]

Dominguez DC. Calcium signalling in bacteria. Mol Microbiol 2004;54:291–297. [PubMed: 15469503]

Eguchi Y, Okada T, Minagawa S, Oshima T, Mori H, Yamamoto K, et al. Signal transduction cascade between EvgA/EvgS and PhoP/PhoQ two-component systems of *Escherichia coli*. J Bacteriol 2004;186:3006–3014. [PubMed: 15126461]

Faruque SM, Albert MJ, Mekalanos JJ. Epidemiology, genetics, and ecology of toxigenic *Vibrio cholerae*. Microbiol Mol Biol Rev 1998;62:1301–1314. [PubMed: 9841673]

Fong JC, Yildiz FH. The *rbmBCDEF* gene cluster modulates development of rugose colony morphology and biofilm formation in *Vibrio cholerae*. J Bacteriol 2007;189:2319–2330. [PubMed: 17220218]

Fong JC, Yildiz FH. Interplay between cyclic AMP-cyclic AMP receptor protein and cyclic di-GMP signaling in *Vibrio cholerae* biofilm formation. J Bacteriol 2008;190:6646–6659. [PubMed: 18708497]

Fong JC, Karplus K, Schoolnik GK, Yildiz FH. Identification and characterization of RbmA, a novel protein required for the development of rugose colony morphology and biofilm structure in *Vibrio cholerae*. J Bacteriol 2006;188:1049–1059. [PubMed: 16428409]

Gotz F. *Staphylococcus* and biofilms. Mol Microbiol 2002;43:1367–1378. [PubMed: 11952892]

Groisman EA. The pleiotropic two-component regulatory system PhoP-PhoQ. J Bacteriol 2001;183:1835–1842. [PubMed: 11222580]

Hammer BK, Bassler BL. Quorum sensing controls biofilm formation in *Vibrio cholerae*. Mol Microbiol 2003;50:101–104. [PubMed: 14507367]

Herrero M, de Lorenzo V, Timmis KN. Transposon vectors containing non-antibiotic resistance selection markers for cloning and stable chromosomal insertion of foreign genes in gram-negative bacteria. J Bacteriol 1990;172:6557–6567. [PubMed: 2172216]

Heydorn A, Ersboll BK, Hentzer M, Parsek MR, Givskov M, Molin S. Experimental reproducibility in flow-chamber biofilms. Microbiology 2000;146:2409–2415. [PubMed: 11021917]

Holland IB, Jones HE, Campbell AK, Jacq A. An assessment of the role of intracellular free Ca^{2+} in *E. coli*. Biochimie 1999;81:901–907. [PubMed: 10572304]

Huq A, Small EB, West PA, Huq MI, Rahman R, Colwell RR. Ecological relationships between *Vibrio cholerae* and planktonic crustacean copepods. Appl Environ Microbiol 1983;45:275–283. [PubMed: 6337551]

Huq A, Huq SA, Grimes DJ, O'Brien M, Chu KH, Capuzzo JM, Colwell RR. Colonization of the gut of the blue crab (*Callinectes sapidus*) by *Vibrio cholerae*. Appl Environ Microbiol 1986;52:586–588. [PubMed: 3767362]

Huq A, Colwell RR, Chowdhury MA, Xu B, Moniruzzaman SM, Islam MS, et al. Coexistence of *Vibrio cholerae* O1 and O139 Bengal in plankton in Bangladesh. Lancet 1995;345:1249. [PubMed: 7739342]

Islam MS, Jahid MI, Rahman MM, Rahman MZ, Islam MS, Kabir MS, et al. Biofilm acts as a microenvironment for plankton-associated *Vibrio cholerae* in the aquatic environment of Bangladesh. Microbiol Immunol 2007;51:369–379. [PubMed: 17446676]

Jones HE, Holland IB, Baker HL, Campbell AK. Slow changes in cytosolic free Ca^{2+} in *Escherichia coli* highlight two putative influx mechanisms in response to changes in extracellular calcium. Cell Calcium 1999;25:265–274. [PubMed: 10378087]

Kaper JB, Morris JG Jr, Levine MM. Cholera. Clin Microbiol Rev 1995;8:48–86. [PubMed: 7704895]

Kierek K, Watnick PI. The *Vibrio cholerae* O139 O-antigen polysaccharide is essential for Ca^{2+}-dependent biofilm development in sea water. Proc Natl Acad Sci USA 2003a;100:14357–14362. [PubMed: 14614140]

Kierek K, Watnick PI. Environmental determinants of *Vibrio cholerae* biofilm development. Appl Environ Microbiol 2003b;69:5079–5088. [PubMed: 12957889]

Lim B, Beyhan S, Meir J, Yildiz FH. Cyclic-diGMP signal transduction systems in *Vibrio cholerae*: modulation of rugosity and biofilm formation. Mol Microbiol 2006;60:331–348. [PubMed: 16573684]

de Lorenzo V, Timmis KN. Analysis and construction of stable phenotypes in gram-negative bacteria with Tn5- and Tn10-derived minitransposons. Meth Enzymol 1994;235:386–405. [PubMed: 8057911]

Minagawa S, Ogasawara H, Kato A, Yamamoto K, Eguchi Y, Oshima T, et al. Identification and molecular characterization of the Mg^{2+} stimulon of *Escherichia coli*. J Bacteriol 2003;185:3696–3702. [PubMed: 12813061]

Norris V, Chen M, Goldberg M, Voskuil J, McGurk G, Holland IB. Calcium in bacteria: a solution to which problem? Mol Microbiol 1991;5:775–778. [PubMed: 1857203]

Norris V, Grant S, Freestone P, Canvin J, Sheikh FN, Toth I, et al. Calcium signalling in bacteria. J Bacteriol 1996;178:3677–3682. [PubMed: 8682765]

Ogasawara H, Hasegawa A, Kanda E, Miki T, Yamamoto K, Ishihama A. Genomic SELEX search for target promoters under the control of the PhoQP-RstBA signal relay cascade. J Bacteriol 2007;189:4791–4799. [PubMed: 17468243]

Patrauchan MA, Sarkisova S, Sauer K, Franklin MJ. Calcium influences cellular and extracellular product formation during biofilm-associated growth of a marine *Pseudoalteromonas* sp. Microbiology 2005;151:2885–2897. [PubMed: 16151201]

Prost LR, Miller SI. The *Salmonellae* PhoQ sensor: mechanisms of detection of phagosome signals. Cell Microbiol 2008;10:576–582. [PubMed: 18182085]

Riley JP, Tongudai M. The major cation/chlorinity ratios in sea water. Chem Geology 1967;2:263.

Romling U, Bian Z, Hammar M, Sierralta WD, Normark S. Curli fibers are highly conserved between *Salmonella typhimurium and Escherichia coli* with respect to operon structure and regulation. J Bacteriol 1998;180:722–731. [PubMed: 9457880]

Rose RK. The role of calcium in oral streptococcal aggregation and the implications for biofilm formation and retention. Biochim Biophys Acta 2000;1475:76–82. [PubMed: 10806341]

Rose RK, Turner SJ. Extracellular Volume in streptococcal model biofilms: effects of pH, calcium and fluoride. Biochim Biophys Acta 1998;1379:185–190. [PubMed: 9528653]

Sarkisova S, Patrauchan MA, Berglund D, Nivens DE, Franklin MJ. Calcium-induced virulence factors associated with the extracellular matrix of mucoid *Pseudomonas aeruginosa* biofilms. J Bacteriol 2005;187:4327–4337. [PubMed: 15968041]

Seputiene V, Motiejunas D, Suziedelis K, Tomenius H, Normark S, Melefors O, Suziedeliene E. Molecular characterization of the acid-inducible *asr* gene of *Escherichia coli and* its role in acid stress response. J Bacteriol 2003;185:2475–2484. [PubMed: 12670971]

Simons RW, Houman F, Kleckner N. Improved single and multicopy lac-based cloning vectors for protein and operon fusions. Gene 1987;53:85–96. [PubMed: 3596251]

Sturn A, Quackenbush J, Trajanoski Z. Genesis: cluster analysis of microarray data. Bioinformatics 2002;18:207–208. [PubMed: 11836235]

Tusher VG, Tibshirani R, Chu G. Significance analysis of microarrays applied to the ionizing radiation response. Proc Natl Acad Sci USA 2001;98:5116–5121. [PubMed: 11309499]

Watnick PI, Kolter R. Steps in the development of a *Vibrio cholerae* El Tor biofilm. Mol Microbiol 1999;34:586–595. [PubMed: 10564499]

Yildiz, FH.; Kolter, R. Genetics and microbiology of biofilm formation by *Vibrio cholerae*. In: Faruque, SM.; Nair, GB., editors. Vibrio Cholerae: Genomics and Molecular Biology. Norfolk, UK: Caister Academic Press; 2008. p. 123-139.

Yildiz FH, Schoolnik GK. *Vibrio cholerae* O1 El Tor: identification of a gene cluster required for the rugose colony type, exopolysaccharide production, chlorine resistance, and biofilm formation. Proc Natl Acad Sci USA 1999;96:4028–4033. [PubMed: 10097157]

Yildiz FH, Dolganov NA, Schoolnik GK. VpsR, a member of the response regulators of the two-component regulatory systems, is required for expression of *vps* biosynthesis genes and EPS(ETr)-associated phenotypes in *Vibrio cholerae* O1 El Tor. J Bacteriol 2001;183:1716–1726. [PubMed: 11160103]

Yildiz FH, Liu XS, Heydorn A, Schoolnik GK. Molecular analysis of rugosity in a *Vibrio cholerae* O1 El Tor phase variant. Mol Microbiol 2004;53:497–515. [PubMed: 15228530]

Zhou L, Lei XH, Bochner BR, Wanner BL. Phenotype microarray analysis of *Escherichia coli* K-12 mutants with deletions of all two-component systems. J Bacteriol 2003;185:4956–4972. [PubMed: 12897016]

Zhu J, Mekalanos JJ. Quorum sensing-dependent biofilms enhance colonization in *Vibrio cholerae*. Dev Cell 2003;5:647–656. [PubMed: 14536065]

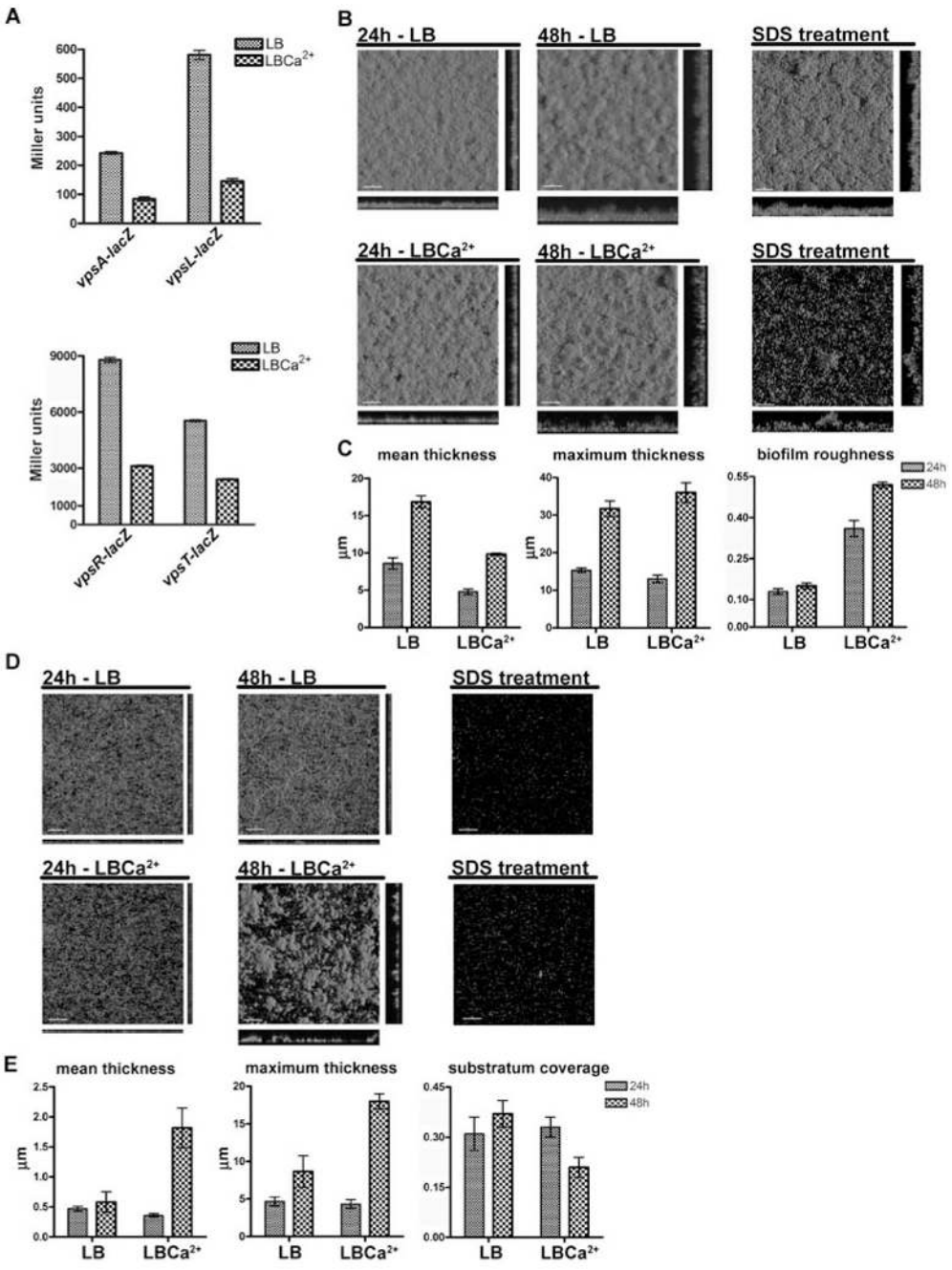

Fig. 1.

Effect of Ca^{2+} on *vps* gene expression and biofilm formation. (A) Comparison of transcription of *vpsA–lacZ*, *vpsL–lacZ*, *vpsR–lacZ* and *vpsT–lacZ* genes as determined by β-galactosidase assay in wild-type cells that were grown to mid-exponential phase in LB and $LBCa^{2+}$ at 30° C. The result shown is the representative of three independent experiments and error bars represent standard deviations. (B, D) Changes in the architecture of the biofilms in response to increase in [Ca^{2+}] in the *gfp*-tagged wild-type cells (B) and Δ*vps* mutant (D). Biofilms of the wild-type cells and Δ*vps* mutant were grown in flow cells for 48 h in LB and $LBCa^{2+}$. Images were acquired at 24 and 48 h time points using a CSLM, and processed using Imaris software. 0.5% SDS was administered into each chamber at a 48 h time point to test biofilm

stability. White bars represent 30 μm. The result shown is representative of three independent experiments. Quantification of changes in the structural properties of biofilms that were formed by the wild-type cells (C) and by Δ*vps* mutant (E) was performed using COMSTAT. Results shown were calculated from three image stacks that were representative of three independent experiments.

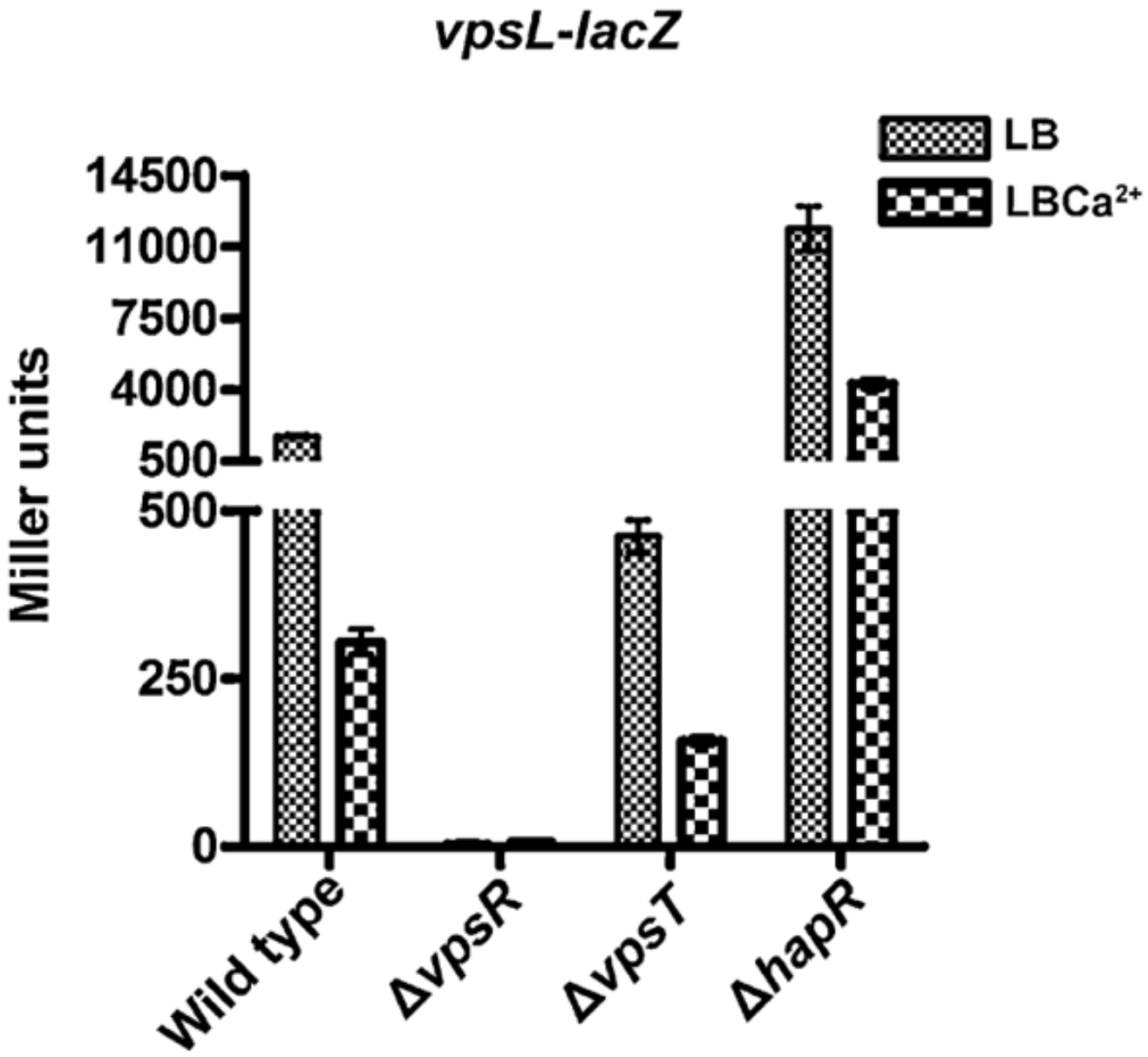

Fig. 2.

Effects of VpsR, VpsT and HapR on Ca^{2+}-mediated repression of *vps* gene expression. Comparison of *vpsL–lacZ* transcription as determined by β-galactosidase assay in wild-type, Δ*vpsR*, Δ*vpsT* and Δ*hapR* strains that were grown to mid-exponential phase in LB and $LBCa^{2+}$ at 30°C. The result shown is the representative of three independent experiments. Error bars represent standard deviation.

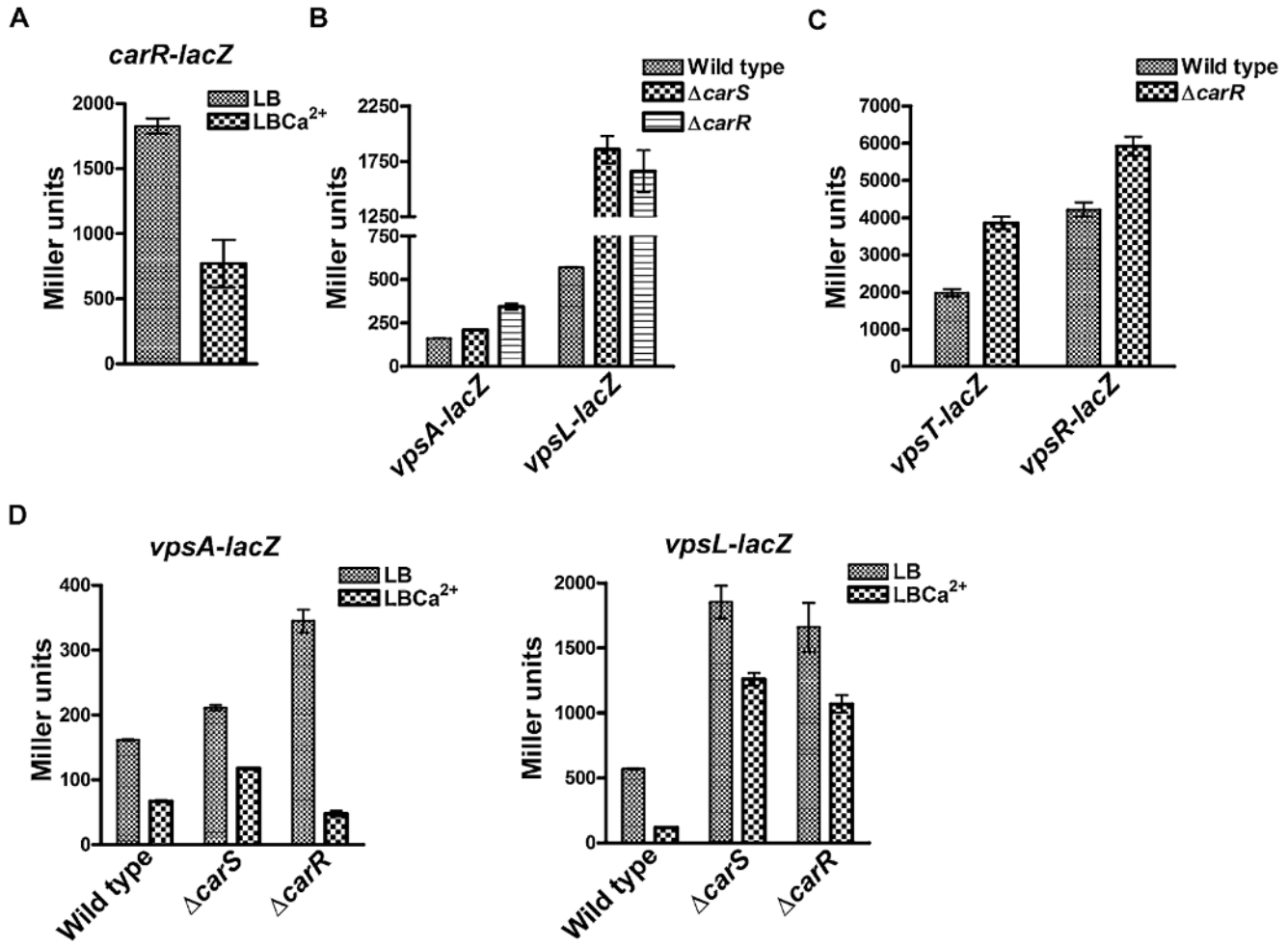

Fig. 3.

CarS and CarR negatively regulate *vps* gene expression.

A. Comparison of transcription of *carR–lacZ* gene, as determined by β-galactosidase assay in wild-type cells that were grown to mid-exponential phase in LB and LBCa^{2+} at 30°C. The result shown is the representative of three independent experiments and error bars represent standard deviations.

B and C. Comparison of *vpsA–lacZ*, *vpsL–lacZ*, *vpsR–lacZ* and *vpsT–lacZ* gene expression as determined by β-galactosidase assay in the wild-type, Δ*carS* or Δ*carR* strains that were grown to mid-exponential phase in LB. The result shown is the representative of three independent experiments and error bars represent standard deviations.

D. Comparison of *vpsA–lacZ* and *vpsL–lacZ* gene expressions in the wild-type, Δ*carR* and Δ*carS* strains that were grown in LB and LBCa^{2+} at 30°C. The result shown is the representative of three independent experiments and error bars represent standard deviation.

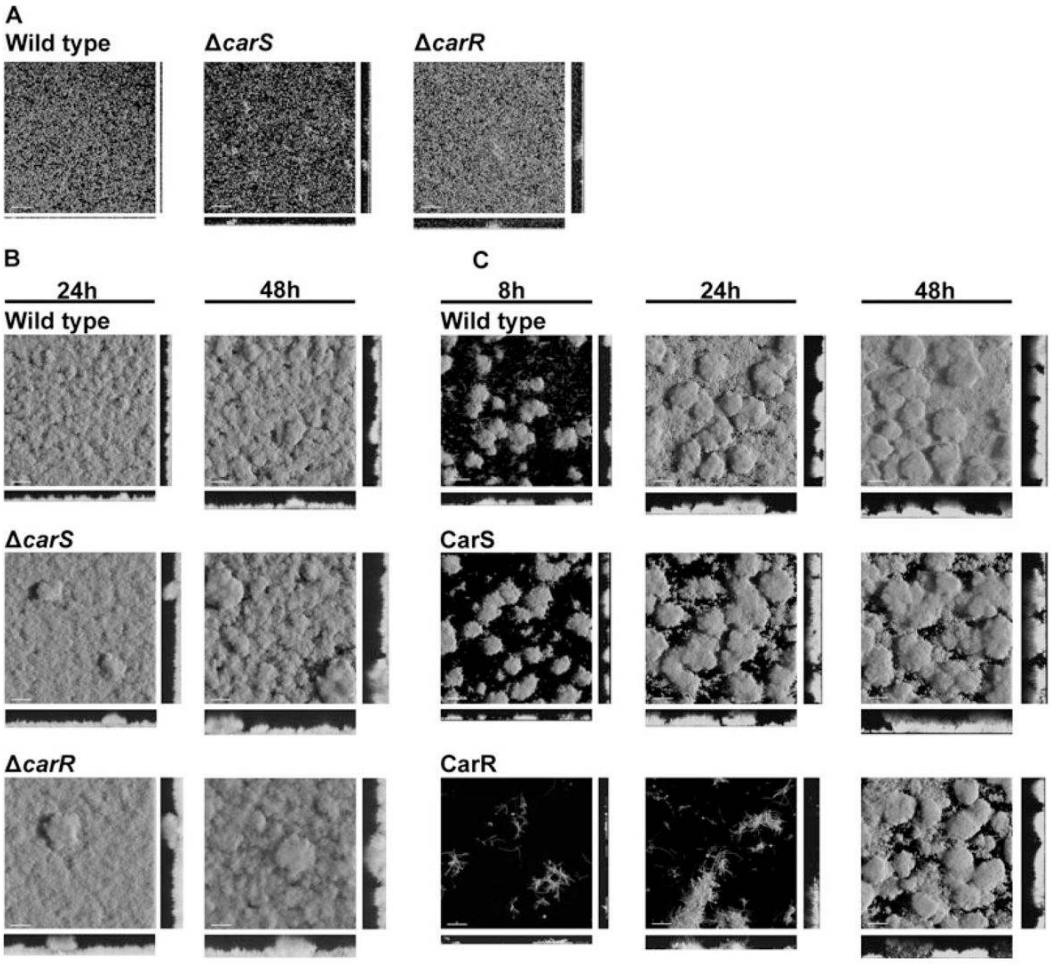

Fig. 4.

Comparison of biofilms of the wild-type, Δ*carS* and Δ*carR* mutant strains.

A. Biofilm structures of the *gfp*-tagged wild-type, Δ*carS* and Δ*carR* strains that were grown under non-flow static conditions. Biofilms were grown in chambered cover-slides for 8 h at 30°C, images were acquired using a CSLM and processed using Imaris software. White bars represent 30 μm. The result shown is representative of three independent experiments.

B. Biofilm structures of the *gfp*-tagged wild-type, Δ*carS* and Δ*carR* strains in a flow-cell system. Biofilms were grown in flow cells for 48 h in LB. Biofilm images were acquired 24 and 48 h after the inoculation using a CSLM and processed using Imaris software. The result shown is representative of three independent experiments. White bars represent 30 μm.

C. Biofilm structures of the *gfp*-tagged wild-type strains harbouring the empty vector pBAD/*Myc*-His C (wild-type), and overexpression plasmids for *carS* (CarS) and *carR* (CarR) in the flow-cell system. Biofilms were grown in flow cells for 48 h in LB supplemented with 0.2% arabinose. Images were taken 8, 24 and 48 h after the inoculation. White bars represent 30 μm. Images were acquired using a CSLM and processed using Imaris software. The result shown is representative of three independent experiments.

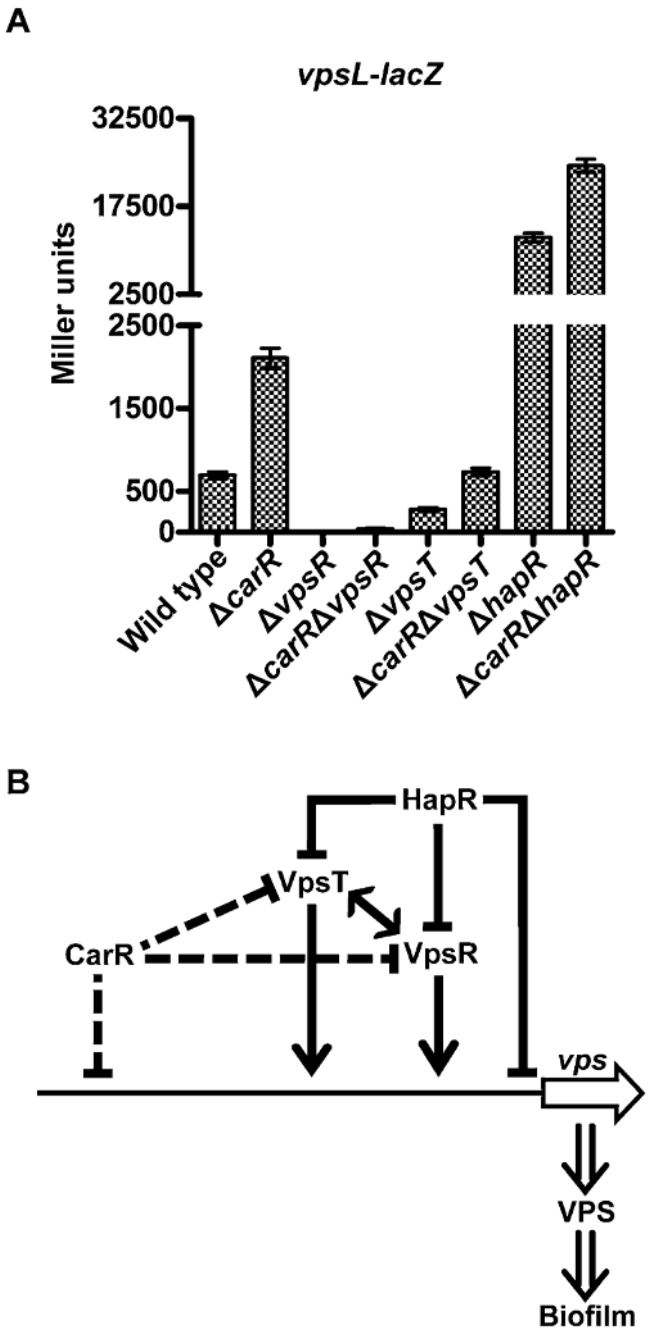

Fig. 5.

Epistasis analysis of *carR*, *vpsR*, *vpsT* and *hapR*.

A. Comparison of transcription of *vpsL–lacZ* as determined by β-galactosidase assay in the wild-type, Δ*carR*, Δ*vpsR*, Δ*vpsR*Δ*carR*, Δ*vpsT,* Δ*vpsT*Δ*carR*, Δ*hapR* and Δ*hapR*Δ*carR* strains that were grown to mid-exponential phase in LB at 30°C. The results shown are representatives of three independent experiments and error bars represent standard deviations.

B. A model of CarR regulation of biofilm formation in *V. cholerae*. Expression of *vps* structural genes, *vpsR* and *vpsT* is negatively regulated by CarR. CarR acts in parallel pathway with HapR.

Table 1

Selected genes that are differentially expressed in wild-type (Wt) grown in $LBCa^{2+}$.[a]

ORF	Gene	Predicted function	Wt-Ca^{2+}/Wt
Biofilm matrix production			
VC0916	*vpsU*	Phosphotyrosine protein phosphatase	0.42
VC0917	*vpsA*	UDP-N-acetylglucosamine 2-epimerase	0.52
VC0918	*vpsB*	UDP-N-acetyl-D-mannosaminuronic acid dehydrogenase	0.36
VC0920	*vpsD*	VPS biosynthesis protein D	0.54
VC0926	*vpsJ*	VPS biosynthesis protein J	0.60
VC0928	*rbmA*	Rugosity and biofilm structure modulator A	0.43
VC0930	*rbmC*	Rugosity and biofilm structure modulator C	0.41
VC0933	*rbmF*	Rugosity and biofilm structure modulator F	0.56
VC1888	*bap1*	Biofilm-associated protein 1	0.47
Pathogenesis			
VC0828	*tcpA*	TCP biosynthesis protein A	3.42
VC0829	*tcpB*	TCP biosynthesis protein B	1.87
VC0830	*tcpQ*	TCP biosynthesis protein Q	2.02
VC0831	*tcpC*	TCP biosynthesis outer membrane protein	2.27
VC0832	*tcpR*	TCP biosynthesis protein R	2.93
VC0833	*tcpD*	TCP biosynthesis protein D	2.31
VC0834	*tcpS*	TCP biosynthesis protein S	2.00
VC0835	*tcpT*	TCP biosynthesis protein T	2.23
VC0836	*tcpE*	TCP biosynthesis protein E	2.07
VC0838	*toxT*	TCP pillus virulence regulatory protein	2.44
VC1456	*ctxB*	Cholera enterotoxin, B subunit	2.21
VC1457	*ctxA*	Cholera enterotoxin, A subunit	2.66
Regulatory proteins			
VC0665	*vpsR*	σ-54-dependent transcriptional regulator	0.63
VC1319	*carS*	Sensor histidine kinase	0.62
VC1320	*carR*	DNA-binding response regulator	0.43

[a]Differentially expressed genes were determined using SAM software with ≥ 1.5-fold change in gene expression and ≤ 3% in false discovery rate as criteria.

Table 2

Quantitative analysis of *V. cholerae* biofilms.

	Average thickness (μm)			Maximum thickness (μm)			Substratum coverage			Roughness coefficient		
	8 h	**24 h**	**48 h**	**8 h**	**24 h**	**48 h**	**8 h**	**24 h**	**48 h**	**8 h**	**24 h**	**48 h**
Wild-type	ND	6.43 ± 1.04	11.85 ± 0.40	ND	15.60 ± 1.04	23.70 ± 1.04	ND	0.98 ± 0.01	0.93 ± 0.01	ND	0.28 ± 0.06	0.38 ± 0.02
Δ*carS*	ND	7.65 ± 1.08	13.41 ± 0.75	ND	27.00 ± 2.38	33.90 ± 4.62	ND	0.95 ± 0.03	0.91 ± 0.04	ND	0.24 ± 0.02	0.43 ± 0.14
Δ*carR*	ND	11.31 ± 1.30	14.26 ± 0.46	ND	30.15 ± 4.45	27.90 ± 2.55	ND	0.98 ± 0.01	0.80 ± 0.05	ND	0.31 ± 0.13	0.40 ± 0.02
Wild-type*	1.47 ± 0.23	8.26 ±1.44	15.03 ± 0.48	15.75 ± 3.18	28.80 ± 2.55	40.05 ± 3.04	0.35 ± 0.00	0.96 ± 0.00	0.99 ± 0.01	1.37 ± 0.07	0.69 ± 0.05	0.55 ± 0.06
CarS*	2.34 ± 0.03	8.13 ± 0.30	16.04 ± 1.77	18.45 ± 3.00	31.05 ± 3.00	34.65 ± 3.18	0.35 ± 0.01	0.65 ± 0.03	0.77 ± 0.05	1.33 ± 0.02	0.87 ± 0.00	0.56 ± 0.09
CarR*	0.11 ± 0.02	1.33 ± 0.28	10.59 ± 0.46	10.35 ± 2.55	24.75 ± 3.18	33.75 ± 0.64	0.04 ± 0.00	0.19 ± 0.05	0.76 ± 0.02	1.90 ± 0.01	1.59 ± 0.06	0.60 ± 0.04

Changes in the structural characteristics of biofilms that were shown in Fig. 4 were calculated using COMSTAT. The result shown is the representative of three independent experiments. Standard deviations are given. ND, not determined. The asterisks represent overexpressions.

Table 3
Bacterial strains and plasmids used in this study.

Strain/plasmid	Relevant genotype and phenotype	Source
Escherichia coli strains		
DH5α	F′*endA1 hsdR17 supE44 thi-1 recA1 gyrA96 relA1* Δ (*argF–lacZYA*) *U169* (*Φ*80*lacΔM15*)	Promega
CC118 (λ pir)	Δ *(ara-leu) araD* Δ*lacX74 galE galK phoA20 thi-1 rspE rpoB argE (Am) recA1* λ *pir*	Herrero *et al*. (1990)
S17-1 (λ pir)	Tp^r Sm^r *recA thi pro* $r_K^- m_K^-$ *RP*4:2-Tc:MuKm Tn7 λ *pir*	de Lorenzo and Timmis (1994)
Vibrio cholerae strains		
FY_Vc_1	*V. cholerae* O1 El Tor A1552, Rif^r	Yildiz and Schoolnik (1999)
FY_Vc_237	FY_Vc_1 mTn7-*gfp*, Rif^r Gm^r	Beyhan *et al.* (2006)
FY_Vc_3	FY_Vc_1 Δ*lacZ*, Rif^r	Casper-Lindley and Yildiz (2004)
FY_Vc_3274	FY_Vc_1 Δ*carS*, Rif^r	This study
FY_Vc_3275	Δ*carS* mTn7-*gfp*, Rif^r Gm^r	This study
FY_Vc_3276	Δ*carS* Δ*lacZ*, Rif^r	This study
FY_Vc_3282	FY_Vc_1 Δ*carR*	This study
FY_Vc_3283	Δ*carR* mTn7-*gfp*, Rif^r Gm^r	This study
FY_Vc_3284	Δ*carR* Δ*lacZ*, Rif^r	This study
FY_Vc_3411	FY_Vc_1 Δ*vps*-I Δ*vps*-II, Rif^r	Fong and Yildiz (2008)
FY_Vc_3924	FY_Vc_1 Δ*vps*-I Δ*vps*-II mTn7-*gfp*, Rif^r	This study
FY_Vc_2874	FY_Vc_1 Δ*lacZ* Δ*vpsR*, Rif^r	Fong and Yildiz (2008)
FY_Vc_2922	FY_Vc_1 Δ*lacZ* Δ*vpsT*, Rif^r	Fong and Yildiz (2008)
FY_Vc_2919	FY_Vc_1 Δ*lacZ* Δ*hapR*, Rif^r	Fong and Yildiz (2008)
FY_Vc_3912	FY_Vc_1 Δ*lacZ* Δ*vpsR* Δ*carR*, Rif^r	This study
FY_Vc_3915	FY_Vc_1 Δ*lacZ* Δ*vpsT* Δ*carR*, Rif^r	This study
FY_Vc_3917	FY_Vc_1 Δ*lacZ* Δ*hapR* Δ*carR*, Rif^r	This study
Plasmids		
pGP704-sac28	pGP704 derivative; *sacB*, Ap^r	G. Schoolnik
pMCM11	pGP704::mTn7-*gfp*, Gm^r, Ap^r	G. Schoolnik
pUX-BF13	oriR6K helper plasmid, provides the Tn7 transposition function *in trans*, Ap^r	Bao *et al.* (1991)
pBAD/Myc-His-C	Arabinose-inducible expression vector with C-terminal Myc epitope and six-His tags	Invitrogen
pRS415	Promoterless *lacZ* cloning vector for transcriptional fusion studies, Ap^r	Simons *et al.* (1987)
pCC2	pGP704-*sac*28:: Δ*lacZ*, Ap^r	Casper-Lindley and Yildiz (2004)
pFY-132	pGP704-*sac*28:: Δ*carS*, Ap^r	This study
pFY-119	pGP704-*sac*28:: Δ*carR*, Ap^r	This study
pFY-604	pBAD-Myc-His-C::*carS*, Ap^r	This study
pFY-605	pBAD-Myc-His-C::*carR*, Ap^r	This study
pCC11	pRS415 *vpsA* promoter, Ap^r	Casper-Lindley and Yildiz (2004)
pCC12	pRS415 *vpsL* promoter, Ap^r	Casper-Lindley and Yildiz (2004)
pCC10	pRS415 *vpsR* promoter, Ap^r	Casper-Lindley and Yildiz (2004)
pCC25	pRS415 *vpsT* promoter, Ap^r	Casper-Lindley and Yildiz (2004)
pFY-606	pRS415 *carR-carS* promoter, Ap^r	This study

Strain/plasmid	Relevant genotype and phenotype	Source